

Deterministic nanoassembly: Neutral or plasma route?

I. Levchenko and K. Ostrikov^{a)}

School of Physics, The University of Sydney, Sydney New South Wales 2006, Australia

M. Keidar

Department of Aerospace Engineering, University of Michigan, Ann Arbor, Michigan 48109-2140

S. Xu

NIE, Nanyang Technological University, 637616 Singapore, Singapore

(Received 27 February 2006; accepted 11 June 2006; published online 19 July 2006)

It is shown that, owing to selective delivery of ionic and neutral building blocks directly from the ionized gas phase and via surface migration, plasma environments offer a better deal of deterministic synthesis of ordered nanoassemblies compared to thermal chemical vapor deposition. The results of hybrid Monte Carlo (gas phase) and adatom self-organization (surface) simulation suggest that higher aspect ratios and better size and pattern uniformity of carbon nanotip microemitters can be achieved via the plasma route. © 2006 American Institute of Physics.

[DOI: 10.1063/1.222249]

Deterministic synthesis of functional nanoassemblies (NAs) ranging from common nanostructures to intricate nanopatterns and nanodevices is a current demand of modern nanoscience and nanotechnology.¹ At the macroscopic level, this implies the ability to select and adjust the process parameters to achieve the desired properties of individual NAs, such as their positioning, alignment, shape, elemental composition, crystallinity, etc.²⁻⁴ At the microscopic level, the determinism implies a certain degree of control over the building blocks (BBs) that self-assemble into the required nanoassemblies and optimization of elementary processes in the nanofabrication environment.⁵ Therefore, the choice of the most favorable environment, which should be dictated by the expected NA parameters, turns out to be a critical factor to reduce process costs and achieve the long-held but as yet elusive goal of deterministic nanofabrication. In this letter, from the microscopic-level viewpoint, we argue that partially ionized environments of the plasma-enhanced chemical vapor deposition⁶ (PECVD) can offer a better deal of controlling the size, shape, and pattern uniformity in deterministic synthesis of selected nanoassemblies, as compared to charge-neutral thermal CVD. To demonstrate this, our target here will be conical carbon nanotip microemitter structures (a representative scanning electron micrograph is shown in Fig. 1) that ideally should have the highest possible aspect (height to width) ratio for higher electron emission yield.⁷ Here, by using a hybrid Monte Carlo (gas phase) and adatom self-organization (surface) simulation, we show that the ionized gas environment is decisive in sustaining the growth of tall and sharp nanotip structures as opposed to short and wide nanotips grown by the CVD under the same process conditions.

The existing relevant numerical efforts are mostly limited to quite separate modeling of plasma composition and (macroscopic) ion fluxes and atomistic configurations of carbon nanotips and relevant films and structures.⁸⁻¹² In the multiscale simulation of our interest here, we combine the motion of neutral and ionic building blocks in the partially ionized gas phase^{13,14} and the growth of the nanotips by ada-

tom and adion insertion via surface migration and directly from the gas phase. We also show that developing conical nanostructures selectively focus ionic building blocks onto their lateral surfaces effectively excluding them from migration over open substrate areas. This results in faster growth rates and eventually in sharper and longer nanotips grown by the PECVD. In our simulations, we have used a system consisting of a biased substrate with the conductive nanotip pattern exposed to the plasma sheath of thickness λ_s . A uniform flux of neutrals and ions is deposited onto the lateral surfaces of the nanotips and substrate areas between the nanotips, for simplicity referred to as open surface areas. The ionization degree of the partially ionized plasma was varied in simulations to relate our numerical results to a broad range of plasma-aided nanofabrication facilities, from weakly ionized RF plasmas¹⁵ of hydrocarbon-based gas mixtures to carbon anodic arcs. For simplicity, only neutral and ionic carbon species have been considered as plasma-generated NA building blocks in our simulations. The plasma ions enter the near-substrate collisionless sheath area with the Bohm velocity $v_0 = (T_e/m_i)^{1/2}$ and then are accelerated to the energy U_s , which includes the initial ion energy at the sheath border, and the gained energy equivalent to the external dc bias applied to the substrate. Here, m_i is the ion mass, and T_e is the electron temperature in electron volts. Under low-bias conditions, one can assume that the sheath width is equal to a few Debye lengths, i.e., $\lambda_s = k(T_e \epsilon_0 / e n_p)^{1/2}$, where n_p is the plasma density, ϵ_0 is the electric constant, and k is the sheath width adjustment coefficient.

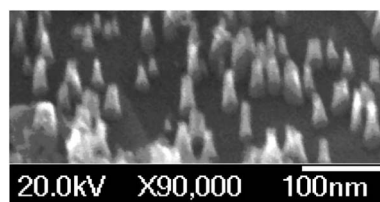


FIG. 1. Representative SEM micrograph of conical carbon nanotips grown by PECVD in Ar+H₂+CH₄ gas mixture on Ni-catalyzed Si(100) (Ref. 20).

^{a)}Electronic mail: k.ostrikov@physics.usyd.edu.au

In numerical simulations, we adopted a multiscale model that simultaneously incorporates the ion motion in the sheath (spatial scales from a few millimeters down to a few hundreds of nanometers), in the vicinity of conducting nanotips (a few hundred down to a few tens nanometers) and adatom migration over open substrate areas (with spatial scales of a few tens to a few nanometers). The code comprises the ion dynamics¹⁴ and surface self-organization¹⁶ numerical modules. Within the ion dynamics module, the ion motion was simulated by using the ion motion equation. The effective electric field acting on an ion at any spatial point was calculated by summation of the microscopic fields of all nanotips in the simulation domain. In this work we use a simplified model of the nanotip growth on nickel-catalyzed Si(100) surface.¹⁵ The growth simulation starts from a small nanotip nucleus. It is assumed that the outer carbon layers of the growing nanotips are able to accommodate insertion of adatoms arriving to the nanotip base from the open surface areas and adions landing directly onto the lateral surfaces from the ionized gas phase. This simple model is an adequate representation of the dynamic growth of various carbon nanofilms and nanostructures that involve hydrogen-terminated surfaces.^{5,7–10,15} The surface self-organization module incorporates the following processes: surface diffusion of adsorbed species to the nanotips, evaporation of adatoms from nanotips to the gas phase and to the two-dimensional vapor, and attachment of adatoms to the nanotip borders. Finally, the module includes a dynamic growth and reshaping of the nanotips, which is described by

$$(\partial V_n / \partial r_{on}) dr_{on} = J_{sn} dt, \quad (1)$$

$$(\partial V_n / \partial h_n) dh_n = J_{en} dt, \quad (2)$$

where V_n , r_{on} , and h_n are the volume, base radius, and height of n th nanotip, respectively. Here, J_{en} is the combined flux of ions and neutrals from the plasma bulk to the n th nanotip lateral surface, J_{sn} is the total surface flux of adatoms to the nanotip's border, and $\partial V_n / \partial r_{on} = (2/3)\pi r_{on} h_n$ and $\partial V_n / \partial h_n = (2/3)\pi r^2$ are the shape- and size-dependent nanotip growth functions in the radial and vertical directions. It is thus assumed that the influx of adsorbed species to the border of each individual nanotip causes an increase in its radius, whereas the direct influx from the ionized gas phase leads to an increase in the nanotip's height.

The simulation starts from the preset pattern of 400 nanotip nuclei covering the simulation area of $S = 1 \times 1 \mu\text{m}^2$. As the height and radius of the nuclei increase, they reshape to the conical nanotips of our interest here. In computations, we used the following parameters: plasma density $n_p = 10^{17}, \dots, 3 \times 10^{18} \text{ m}^{-3}$, electron energy 2–5 eV, $U_S \approx 20\text{--}50 \text{ V}$, surface temperature $T_S \approx 750 \text{ K}$, gas temperature $T_G \approx 1000 \text{ K}$, and gas pressure $P_G \approx 1 \text{ Pa}$. This set of parameters is representative to PECVD of carbon nanotip structures in RF plasmas.^{5,10,15} The microscopic topography

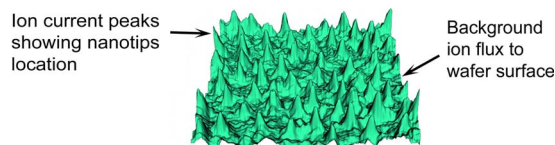


FIG. 2. (Color online) Three-dimensional topology of the ion current over the simulated nanopattern.

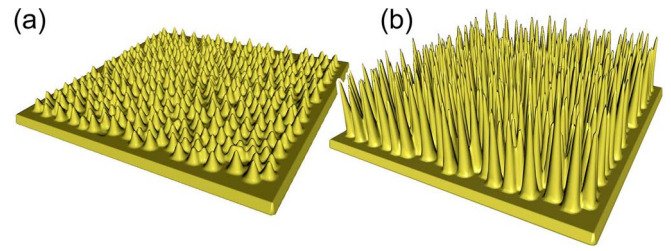


FIG. 3. (Color online) Developed carbon nanotip patterns (a) grown by CVD and (b) grown by PECVD in a plasma with $n_p = 3.0 \times 10^{18} \text{ m}^{-3}$. In both cases, the simulation was terminated when the coverage reached $\mu = 0.70$.

of the ion flux on open surface areas and nanotip lateral surfaces was simulated by a Monte Carlo method. An initial surface coverage μ_0 was 0.1, a typical value in the low surface coverage case.

A representative three-dimensional distribution of the ion current density on the nanostructured substrate surface is shown in Fig. 2. The positions of individual carbon nanotips can be easily identified as well-pronounced sharp ion current peaks, surrounded by the significantly reduced background ion flux onto open surface areas. Evidently, the simulated three-dimensional (3D) ion current distribution suggests an enhanced influx of the building blocks directly to the nanotip lateral surfaces, without allowing them to deposit on open surface areas and migrate to nanotip borders over the surface. Furthermore, as our results suggest, such strongly focused microscopic pattern of the ion deposition enables one to control the growth rates and aspect ratios of the nanostructures.

A striking observation made in our numerical experiments is depicted in Fig. 3, which suggests that the nanotips grown on plasma-exposed surfaces [Fig. 3(b)] are much taller and sharper than those grown by the CVD process [Fig. 3(a)] under the same deposition conditions. To quantify this main conclusion, we studied the dependence of the mean nanotip apex angle α and mean nanotip height h_m on the mean nanotip radius (Fig. 4) with the plasma density as a parameter. Another important feature of the development of the nanotip array is an essentially different behavior of the apex angle at the initial and developed growth stages. Specifically, an initial increase of the apex angle is followed by its gradual decrease resulting in nanotip sharpening with time. This phenomenon may be explained as follows. When the nanotip height is small, the nonuniformity of the electric field is weak to focus the ion current onto the nanotip lateral surfaces, and the ionic building blocks are mostly deposited to open surface areas where they are neutralized and become adatoms. In this case the nanotip growth is maintained mostly by the adatom BBs migrating to nanotip borders over the surface. As a result, the nanotip base radius increases rapidly, with the height increasing slowly. When the nanotips

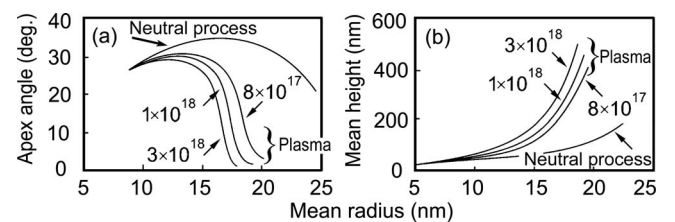


FIG. 4. Dependence of the nanotip apex angle (a) and mean height (b) on their mean radius for the neutral and plasma-aided processes with the plasma density (m^{-3}) as a parameter.

become higher, the ion current is focused by nonuniform electric fields and thus is increasingly diverted to their lateral surfaces. This causes, in turn, a noticeable decrease in the apex angle. This effect turns out to be more pronounced in denser plasmas, and the sharpest nanotips in our numerical experiments have been observed for $n_p = 3 \times 10^{18} \text{ m}^{-3}$.

Indeed, higher plasma densities result in more efficient precipitation of the ionic BBs on the nanotip surfaces. This also results in smaller sheath widths and more focused ion deposition onto the upper sections of the nanostructures, closer to their crests. Our results also suggest that one can achieve aspect ratios of more than 30 by using the PECVD route. On the contrary, the CVD process can offer the nanotip aspect ratios not exceeding 20 under the same conditions. Moreover, dynamic changes of the nanotip aspect ratios turn out to be more pronounced in the plasma-aided process. In other words, a chance of an initial nanotip nucleus to evolve as a sharp, high-aspect-ratio nanocone is much higher on plasma-exposed surfaces.

It is noteworthy that our “macroscopic” model does not include atomic forces and interactions of individual atoms and is based on physical evaporation of adions and adatoms in and out of the growing conical nanotip structures. The model builds on the established, commonly used, well proven, and justified principles and approaches of surface science to surface diffusion phenomena and island nucleation and growth.^{17,18} In this letter these models have been advanced by involving individual treatment of the growth process of 400 “macroscopic” nanotips (each containing approximately 1.5–2 million atoms) arranged in an ordered array on the plasma-exposed surface. Moreover, our hybrid multiscale simulation bridges processes occurring at length scales different by several orders of magnitude and involves a very large number of atoms and ions, which is far beyond the capabilities of the present-day *ab initio* atomic-level numerical techniques, such as the molecular dynamics (MD) of density functional theory (DFT) approaches. Therefore, atomistic models would only offer a better deal of accuracy in considering the growth of individual nanostructures with the substantially reduced number (typically not exceeding a few hundred) of atoms. We emphasize that a number of recent experimental and computational results corroborate the fidelity of the chosen nanotip growth model. These include (i) scanning electron microscope (SEM) analysis of the nanotip shapes at different growth stages (see, e.g., Fig. 1 and Refs. 11 and 15), (ii) experimental evidence of the nanotip sharpening when a dc bias is applied to the substrate,^{11,15} (iii) transmission electron microscopy (TEM) of carbon nanotips made of parallel graphite layers and terminated by hydrogen on lateral surfaces¹¹ and made of stacked conical sheets¹⁹ showing that the nanotips are crystalline and fully filled by carbon atoms and have apex angles ($\sim 5^\circ - 9^\circ$) and geometrical sizes very similar to the results of our numerical simulations [see, e.g., Fig. 3(b)], and (iv) results of *ab initio* DFT computations showing that (substantially downscaled) nanotips made of parallel graphite layers and terminated by hydrogen on lateral surfaces is a stable atomic configuration.¹¹

Our results thus suggest that the plasma-aided process, in contrast to the neutral flux deposition, is a very efficient tool to control the nanotip aspect ratio, a critical factor in microemitter array applications. These two important factors

can be controlled by adjusting the plasma parameters such as the degree of ionization, plasma density, electron temperature, etc. Physically, a certain degree of determinism in the plasma-assisted synthesis of carbon nanotips can be achieved by properly manipulating the two building block delivery channels: via surface migration and directly from the ionized gas phase. It becomes evident that an increased influx and controllable deposition of ionic BBs directly onto the nanotip lateral surfaces can be used to deterministically control the geometric shape of the nanotips.

This work primarily aimed to show the advantages offered by the plasma-aided nanoassembly in controlling the growth and shape of the nanostructures rather than exploring the detailed parameter ranges where such control is most efficient. Other benefits of plasma-aided nanofabrication compared to neutral gas-based techniques, such as generation of the BBs in the required energetic and chemical states, nanomanipulation of BBs by using various forces in the plasma sheath, electric field-controlled alignment of nanoassemblies, surface-charge controlled self-organization on plasma-exposed surfaces, and several others, are discussed elsewhere.^{5,7–10} Fundamentally, plasma-aided nanofabrication simultaneously involves two main approaches of modern nanoscience, namely, nanomanipulation (by the electric field) and self-organization (including migration on plasma exposed surfaces and self-assembly) of building blocks.

¹Nanotechnology: Shaping the World Atom by Atom, National Science and Technology Council, 1999; <http://www.nano.gov>

²K. Kang, L. H. Lewis, and A. R. Moodenbaugh, *Appl. Phys. Lett.* **87**, 062505 (2005).

³H. C. Lo, D. Das, J. S. Hwang, K. H. Chen, C. H. Hsu, C. F. Chen, and L. C. Chen, *Appl. Phys. Lett.* **83**, 1420 (2003).

⁴Y. H. Wang, M. J. Kim, H. W. Shan, C. Kittrell, H. Fan, L. M. Ericson, W. F. Hwang, S. Arepalli, R. H. Hauge, and R. E. Smalley, *Nano Lett.* **5**, 997 (2005).

⁵K. Ostrikov, *Rev. Mod. Phys.* **77**, 489 (2005).

⁶I. Levchenko, M. Romanov, M. Keidar, and I. Beilis, *Appl. Phys. Lett.* **85**, 2202 (2004).

⁷A. V. Melechko, V. I. Merkulov, T. E. McKnight, M. A. Guillorn, K. L. Klein, D. H. Lowndes, and M. L. Simpson, *J. Appl. Phys.* **97**, 041301 (2005).

⁸K. B. K. Teo, D. B. Hash, R. G. Lacerda, N. L. Rupasinghe, M. S. Bell, S. H. Dalal, D. Bose, T. R. Govindan, B. A. Cruden, M. Chhowalla, G. A. J. Amaratunga, M. Meyyappan, and W. I. Milne, *Nano Lett.* **4**, 921 (2004).

⁹M. S. Bell, R. G. Lacerda, K. B. K. Teo, N. L. Rupasinghe, G. A. J. Amaratunga, W. I. Milne, and M. Chhowalla, *Appl. Phys. Lett.* **85**, 1137 (2004).

¹⁰I. B. Denysenko, S. Xu, P. P. Rutkevych, J. D. Long, N. A. Azarenkov, and K. Ostrikov, *J. Appl. Phys.* **95**, 2713 (2004).

¹¹K. Ostrikov, J. D. Long, P. P. Rutkevych, and S. Xu, *Vacuum* (to be published); S. Xu, K. Ostrikov, J. D. Long, and S. Y. Huang, *Vacuum* **80**, 621 (2006).

¹²D. B. Hash, M. S. Bell, K. B. K. Teo, B. A. Cruden, W. I. Milne, and M. Meyyappan, *Nanotechnology* **6**, 925 (2005).

¹³I. Levchenko, M. Korobov, M. Romanov, and M. Keidar, *J. Phys. D* **37**, 1690 (2004).

¹⁴I. Levchenko, K. Ostrikov, M. Keidar, and S. Xu, *J. Appl. Phys.* **98**, 064304 (2005).

¹⁵Z. L. Tsakadze, K. Ostrikov, J. D. Long, and S. Xu, *Diamond Relat. Mater.* **13**, 1923 (2004); Z. L. Tsakadze, K. Ostrikov, and S. Xu, *Surf. Coat. Technol.* **191**, 49 (2005).

¹⁶I. Levchenko and O. Baranov, *Vacuum* **72**, 205 (2004).

¹⁷J. V. Barth, *Surf. Sci. Rep.* **40**, 75 (2000).

¹⁸F. Rosei and R. Rosei, *Surf. Sci.* **500**, 395 (2002).

¹⁹G. Zhang, X. Jiang, and E. Wang, *Science* **300**, 472 (2003).

²⁰Z. L. Tsakadze, K. Ostrikov, and S. Xu (unpublished).